Hindawi
Advances in Polymer Technology
Volume 2024, Article ID 8747902, 14 pages
https://doi.org/10.1155/2024/8747902

Research Article

Design of Highly Porous Materials Based on Chitosan/Pectin Interpolyelectrolyte Complex for Wound Healing Application

Aliaksandr Kraskouski,[1] **Maksim Mashkin**,[1] **Viktoryia Kulikouskaya**,[1] **Viktoryia Savich**,[2] **Anastasiya Sidarenka**,[2] **Sergei Pinchuk**,[3] **and Ruibin Li**[4]

[1]*Institute of Chemistry of New Materials of the National Academy of Sciences of Belarus, 36 F. Skaryna Str., Minsk 220084, Belarus*
[2]*Institute of Microbiology of the National Academy of Sciences of Belarus, 2 Kuprevich Str., Minsk 220084, Belarus*
[3]*Institute of Biophysics and Cell Engineering of the National Academy of Sciences of Belarus, 27 Academicheskaya Str., Minsk 220072, Belarus*
[4]*State Key Laboratory of Radiation Medicine and Protection, School for Radiological and Interdisciplinary Sciences (RAD-X), Collaborative Innovation Center of Radiological Medicine of Jiangsu Higher Education Institutions, Suzhou Medical College, Soochow University, Suzhou 215123, Jiangsu, China*

Correspondence should be addressed to Aliaksandr Kraskouski; aleks.kraskovsky@gmail.com

Received 24 November 2023; Revised 3 April 2024; Accepted 26 April 2024; Published 9 May 2024

Academic Editor: Alain Durand

Interpolyelectrolyte complexes (IPECs) of polysaccharides are multifunctional polymer materials that improve the mechanical and physicochemical properties of individual polysaccharides. In this study, highly porous (>90%) materials based on IPECs of versatile natural polysaccharides, chitosan (30 and 1,200 kDa) and pectin, are obtained by freeze-drying technique. To enhance the interaction between chitosan and pectin macromolecules, the latter are chemically functionalized with dialdehyde groups. The chitosan-/aldehyde-functionalized pectin (Chit/AF-Pect) polyelectrolyte complex sponges obtained are characterized using SEM, FTIR spectroscopy, and TGA. The swelling capacity study reveals a higher swelling ratio of IPEC sponges with an increase in both the molecular weight and content of chitosan: for Chit30/AF-Pect, the swelling ratio rises from 327% to 480%, while for Chit1200/AF-Pect, from 681% to 1,066%. Additionally, the in vitro degradation test demonstrates higher stability of Chit1200/AF-Pect sponges in comparison with those of Chit30/AF-Pect: after 4 days of incubation, the weight losses are found to be 9%–16% and 18%–41%, respectively. The cytotoxicity study shows that Chit30/AF-Pect sponges are noncytotoxic, with cell viability values >70%. Furthermore, the Chit30/AF-Pect sponges, obtained at chitosan:pectin weight ratio of 5:1, exhibit bactericidal activity against *Escherichia coli* BIM B-984 G, *Pseudomonas aeruginosa* BIM B-807 G, *Staphylococcus aureus* BIM B-1841, and slightly inhibit the growth of *Enterococcus faecalis* BIM B-1530 G. These findings indicate that the obtained Chit30/AF-Pect sponges can be used to create wound dressings for wound healing applications.

1. Introduction

Purulent-necrotizing soft tissue infections are a serious life-threatening problem in surgery due to the emergence of multidrug resistance in pathogenic bacteria [1]. The necrotizing infections cause tissue death and are clinically characterized by high morbidity and mortality [2]. Wound dressings are commonly used to support the numerous phases of the wound repair by covering the surface of damaged tissue [3, 4]. The main characteristics for wound dressings include biocompatibility, nontoxicity, absence of local irritant and allergic reactions, maintaining the environment moist, oxygen and water vapor permeability, high adsorption capacity, ability to prevent the penetration of microorganisms, and others [4, 5]. A promising approach for developing wound dressings involves utilizing biologically active natural polymers [6], including polysaccharides. These biopolymers display potential for regenerative medicine applications [7–9], as they can be utilized during different stages of the wound healing process [3, 7]. Given the ease availability, nontoxic nature, biocompatibility, biodegradability, wide range of biological properties, and

wide application prospects of polysaccharides [6, 10], wound dressings utilizing these polymers can prove to be a highly effective way to improve and accelerate wound healing, including in cases of purulent-necrotic wounds [3, 5, 7]. The natural polysaccharides chitosan and pectin are among the most attractive for wound healing applications.

Chitosan is a linear polycationic polysaccharide composed of randomly distributed β-(1→4)-linked D-glucosamine (deacetylated unit) and N-acetyl-D-glucosamine (acetylated unit). This biopolymer is considered generally recognized as safe (GRAS) and has antifungal [11, 12], antibacterial [11, 13], hemostatic [14, 15], mucoadhesive [16, 17], and other [18] properties. Therefore, chitosan-based materials have been widely utilized in tissue engineering [19], drug delivery systems [20, 21], and wound healing [4, 22]. Pectin is a natural polysaccharide composed of (1→4)-linked α-D-galacturonic acid residues containing 2-O-substituted L-rhamnopyranose residues. Pectin exhibits diverse physiological activities, including anti-inflammatory [23], mucoadhesive [24], antibacterial [25], anti-ulcer [26], and other [27] properties. Pectin-based biomaterials have gained popularity in the biomedical field [28, 29] and are being considered for use as innovative wound dressings for effective healing [30].

However, pure polysaccharide materials lack the strength, flexibility, stability, etc. Therefore, to improve the mechanical and physicochemical properties of polysaccharide materials, they can be blended with other natural or synthetic polymers [28, 31]. Khorshidi et al.[32] reported that functionalized pectin/fibroin compositions had superior mechanical properties compared to either neat fibroin or functionalized pectin and preserved the viability of rabbit stem cells. One of the promising polymer-blended formulations is the interpolyelectrolyte complexes (IPECs). IPECs are multifunctional polymer materials formed by electrostatic interactions between oppositely charged polyelectrolytes [33, 34]. IPECs possess unique physicochemical properties that differ significantly from those of the original polymers. Kulig et al. [35] prepared alginate–chitosan polyelectrolyte complexes and showed that the properties of the polysaccharides complement each other: mixing sodium alginate with chitosan improves its flexibility, and chitosan within an IPEC provides thermal resistance. Chitosan, as the only naturally occurring cationic polysaccharide, can readily form IPECs with a range of anionic polyelectrolytes, including pectin [36], sodium alginate [35], hyaluronic acid [37], carboxymethyl cellulose [38], gelatin [39], and others [40]. Polysaccharide-based polyelectrolyte complexes have been investigated as novel platforms in drug delivery systems [41, 42], tissue engineering [43, 44], and wound healing applications [45, 46].

The objective of this study was to fabricate porous materials based on IPECs of chitosan and pectin via freeze-drying. Furthermore, the physicochemical properties, cytotoxicity, and antibacterial activity of these materials against Gram-positive and Gram-negative bacteria were evaluated to determine their potential as wound dressings.

2. Materials and Methods

2.1. Materials. Low molecular weight chitosan (Chit30, $M_w \sim 30$ kDa, degree of deacetylation >90%) was purchased from Glentham Life Sciences (UK). High molecular weight chitosan (Chit1200, $M_v \sim 1{,}200$ kDa, degree of deacetylation >75%) was procured from Sigma–Aldrich (Germany). Pectin (Pect, degree of esterification 35%–42%, $M_v \sim 89{,}000$) was obtained from Herbstreith & Fox (Germany). Sodium (meta) periodate (≥99%, $M_w = 213.89$) was purchased from Sigma–Aldrich (Germany). The other used reagents (ethylene glycol, ethanol, acetic acid, borax, Lugol's iodine, hydrochloric acid, sodium thiosulfate, and starch) from commercial sources were analytical grade and employed without future purification. All aqueous solutions were prepared with distilled water.

2.2. Synthesis of Aldehyde-Functionalized Pectin (AF-Pect). The oxidation of pectin to form aldehyde groups was carried out according to the method proposed by Patenaude and Hoare [47] using sodium periodate as the oxidizing agent. Sodium periodate (0.8 g) was added to 150 mL of an aqueous solution of pectin (10 mg/mL) and left under stirring in the dark at room temperature for 16 hr. Then, 0.4 mL of ethylene glycol was added to stop the reaction, and the mixture was stirred for an additional 1.5 hr. The reaction solution was purified by dialysis (cellulose dialysis tubing, 14 kDa, Sigma–Aldrich (Germany)) against water for 3 days. The purified AF-Pect was frozen at −20°C (24 hr) and freeze-dried at −50°C and 4 Pa for 8 hr.

2.2.1. Determination of Iodine Number of AF-Pect. The iodine number of AF-Pect was determined by the following method. First, 10 mL of a 0.05 N borax solution (pH 9.2) was pipetted into a 100-mL Erlenmeyer flask with a ground joint. The flask was then kept in a thermostat at 25.0 ± 1.0°C for 15 min. Next, 20 mL of a 0.03 N (by iodine) Lugol's solution, previously held in the same thermostat, was added. After the contents of the flask were mixed, 0.1 g of the test sample was quickly added. The flask was then sealed with the ground-glass stopper and placed in the thermostat at 25.0 ± 1.0°C, stirring the contents occasionally. After 6 hr, 15 mL of a 0.1 N hydrochloric acid solution was added, and the excess of iodine was back titrated with $a \sim 0.013$ N sodium thiosulfate solution, adding 0.8 mL of a 0.5% starch solution at the end of the titration. A blank value was also measured. The procedure was equal to the test sample measurement but without adding the sample. Iodine number was calculated according to Equation (1):

$$\text{Iodine number} = \frac{(a-b) \times c \times 10 \times 100}{g \times (100-w)}, \quad (1)$$

where a and b are the volumes of sodium thiosulfate solution used for titration of the blank and test samples, respectively, mL; c is the concentration of sodium thiosulfate solution, mol/L; g is the weight of the test sample, g; and w is the

moisture of the test sample (determined by drying to constant weight, %). The data presented were averaged from three measurements.

2.3. Formation of Chitosan/Aldehyde-Functionalized Pectin (Chit/AF-Pect) Polyelectrolyte Complex Sponges. Polysaccharide sponges were obtained according to previously described technique [48] with slight modifications. To form sponges, aqueous solution (2 mL) of oxidized pectin (5, 10, and 15 mg/mL) was quickly added into chitosan (30 and 1,200 kDa) solution (2 mL) in 2% acetic acid (15, 20, and 25 mg/mL) under vigorous shaking on the vortex, and the mixture was left for 1 hr to complete the formation of IPECs. The Chit:AF-Pect weight ratio was 1 : 1, 2 : 1, and 5 : 1. Then, the resulting complexes were poured into 35 mm plastic Petri dishes, cooled at 4°C for 1 hr, and frozen at −20°C. The frozen samples were freeze-dried (Labconco FreeZone 1.0, USA) at −50°C and 4 Pa for 8 hr. Thus, six types of Chit/AF-Pect polyelectrolyte complex sponges were obtained (Chit30/AF-Pect (1 : 1), Chit30/AF-Pect (2 : 1), Chit30/AF-Pect (5 : 1), Chit1200/AF-Pect (1 : 1), Chit1200/AF-Pect (2 : 1), and Chit1200/AF-Pect (5 : 1)) differing in the molecular weight of chitosan used and the weight ratio of Chit:AF-Pect.

2.4. Characterization of Chit/AF-Pect Polyelectrolyte Complex Sponges

2.4.1. Scanning Electron Microscopy (SEM). The morphology of the sponges was examined using a scanning electron microscope (JCM-6000Plus, Jeol, Japan). The samples were covered with platinum, and SEM images were taken with a resolution of 100–200 μm in high vacuum mode at an accelerating voltage of 15 kV. SEM images were analyzed using "JCM-6000 Plus Standard Software ver. 1.6.0."

2.4.2. Density and Porosity Measurements. The density and porosity of the sponges were determined by the liquid displacement method [8]. A sample with a defined weight (W) was immersed in a known volume of ethanol (V_1). The total volume of ethanol and the ethanol-impregnated sponge (V_2) were measured in 5 min. The sample was removed from the solution, and the residual volume of ethanol was determined (V_3). The density of the porous sponge (d) and its porosity (P) were calculated according to Equations (2) and (3):

$$d = \frac{W}{V_2 - V_3}, \tag{2}$$

$$P = \frac{V_1 - V_3}{V_2 - V_3}. \tag{3}$$

The data presented were averaged from two measurements.

2.4.3. Fourier Transform Infrared (FTIR) Spectroscopy. FTIR spectra of Chit/AF-Pect sponges were recorded using Tensor-27 spectrophotometer (Bruker, Germany) by scanning along a spectrum range from 400 to 4,000 cm^{-1}. Data collection was performed with a 4 cm^{-1} spectral resolution and 32 scans.

2.4.4. Thermogravimetric Analysis (TGA). A thermogravimetric analysis was carried out to determine the thermal stability of the Chit/AF-Pect sponges using TGA instrument STA 449 F3 (Netzsch, Germany) under the following conditions: crucible Al_2O_3; temperature range from 25 to 600°C; heating rate, 10 K/min; oxygen/nitrogen atmosphere; and weight of samples, 12–16 mg.

2.4.5. Swelling Capacity. For swelling capacity evaluation, preliminarily weighed samples were immersed in 3 mL of Dulbecco's phosphate-buffered saline (DPBS, pH 7.0–7.5) at room temperature for 1 hr. Then, samples were taken out, and excess moisture was removed by a Schott filter for 5 min. These sponges were then immediately weighed, and the swelling ratio was calculated according to Equation (4):

$$\text{Swelling ratio} = \frac{m - m_0}{m_0 \times 100\%}, \tag{4}$$

where m is the weight of the swollen sponge, mg, and m_0 is the weight of the initial dry sponge, mg. All experiments were carried out in triplicate.

2.4.6. In Vitro Degradation Study. The sponge's degradation was studied in vitro in DPBS (pH 7.0–7.5) at 37°C. The samples of a defined weight were immersed in 10 mL of DPBS, after specific time intervals (1, 2, 3, and 4 days), the sponges were removed from the solution. The excess buffer was removed with filter paper, and the sponges were dried at 50−60°C and weighed. The presented data represents an average of four measurements.

2.4.7. Cytotoxicity toward Mesenchymal Stem Cells (MSCs). The cytotoxicity study of Chit30/AF-Pect sponges towards MSCs was carried out according to the previously described technique [49]. MSCs were isolated from Wistar rat fat homogenate by its enzymatic treatment in collagenase solution. MSCs at passages No. 2 and 3 were used. Immunophenotype of MSCs was confirmed by flow cytometry (FACSCanto II, Becton Dickinson, USA). The obtained cells expressed typical for MSCs CD90 (>95%), CD105 (>99%), CD29 (>90%), and CD44 (>95%) markers. The expression of hematopoietic cell markers was insignificant: CD34 (<3%) and CD45 (<2%).

Chit30/AF-Pect sponges were sterilized by ethylene oxide (Steri-Vac 5XL 3M, USA). To study the cytotoxicity, Chit30/AF-Pect sponges were placed in Petri dishes and hydrated by growth medium (2 mL, Dulbecco's modified Eagle medium, containing 10% fetal bovine serum, 2 mM L-glutamine, and 0.01 mL of the complex antibiotic–antimycotic base solution). After 5 min, sponges were seeded with 1.5 mL of MSC suspension (2×10^5 cells) in growth medium and cultivated at 37°C in the humid air atmosphere with 5% CO_2 for 24 hr.

The viability of MSCs was determined by fluorescence microscopy using fluorescein diacetate (FDA) and propidium iodide (PI) dyes. The microscopy of MSCs in the fluorescence mode was carried out on an inverted Olympus IX71 microscope using a fluorescent filter cube for the green and red regions with fluorescence excitation parameters 420–495 and 520–560 nm and its registration at 505–560

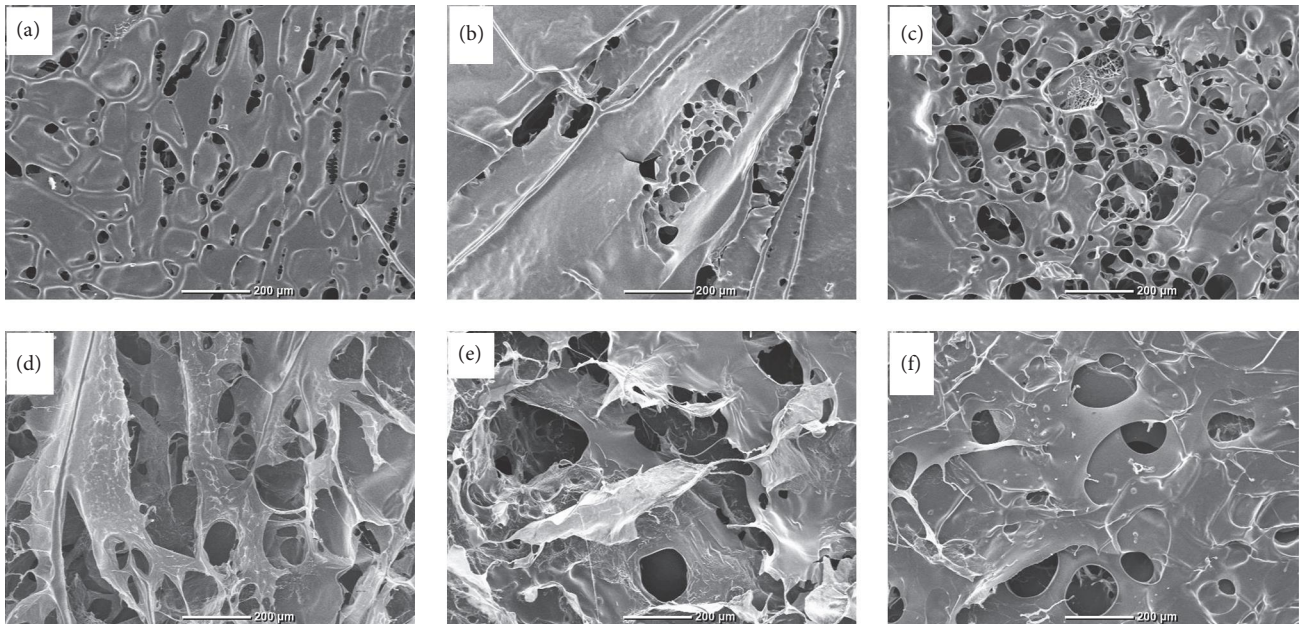

FIGURE 1: SEM images of Chit/AF-Pect (1 : 1) (a and d), Chit/AF-Pect (2 : 1) (b and e), and Chit/AF-Pect (5 : 1) (c and f) sponges. The molecular weight of chitosan was 30 kDa (a–c) and 1,200 kDa (d–f).

and 620–720 nm, respectively. MSCs, cultured on sponges, were stained with FDA (0.5 μg/mL) and PI (5 μg/mL) for 10 min in the dark at room temperature. The fluorescence was registered utilizing a digital camera DP72. The resulting images were analyzed using the Cell F software (Olympus, Japan). Intense fluorescence of cells in the green region of the spectrum (505–560 nm) indicates the high activity of intracellular esterases and the presence of viable cells. Cells in the state of necrosis possess by fluorescence in the red region (620–720 nm).

2.4.8. Antibacterial Activity. The antibacterial activity of Chit/AF-Pect polyelectrolyte complex sponges was assessed against both Gram-negative and Gram-positive bacteria. Bacterial strains *Escherichia coli* BIM B-984 G, *Pseudomonas aeruginosa* BIM B-807 G, *Staphylococcus aureus* BIM B-1841, *Streptococcus pyogenes* BIM B-1529 G, and *Enterococcus faecalis* BIM B-1530 G were obtained from the Belarusian Collection of Non-pathogenic Microorganisms. The bacteria were cultured on Columbia agar (Condalab) at 37°C for 24–48 hr, depending on the strain. Afterward, the bacterial cultures were diluted in physiological saline (0.9% NaCl) to achieve a turbidity of 1.0 McFarland. The bacterial suspensions were then inoculated into flasks containing 9.9 mL of Columbia broth (Condalab). IPEC sponges with a diameter of approximately 32 mm were sterilized using ultraviolet light for 60 min. Following sterilization, the sponges were submerged in flasks containing bacterial inoculum ($\sim 10^6$ CFU/mL) and Columbia broth. Inoculated Columbia broth without sponges was used as the positive control. Noninoculated culture media with or without sponges served as the negative controls. For the comparative experiment, AF-Pect and chitosan sponges prepared using the same freeze-drying technique as IPEC sponges were employed.

The plate count assay was used to determine viable bacterial cell counts at 1, 2, 3, 4, and 24 hr of incubation at 37°C and 180 rpm. To perform the assay, bacterial cultures were serially tenfold diluted in physiological saline, plated on Columbia agar, and then incubated at 37°C for 24–48 hr depending on the strain. The number of bacterial colonies was subsequently counted.

2.5. Statistical Analysis. Results were presented as mean $\pm$ SD. The statistical analysis of the obtained data was performed using the one-way analysis of variance (ANOVA). The value of $p < 0.05$ was considered to be statistically significant.

3. Results and Discussion

To enhance the interaction between chitosan and pectin macromolecules and improve the stability of IPEC sponges in culture media and buffer solutions, pectin macromolecules were chemically functionalized using the sodium periodate oxidation method. Periodate oxidation, which leads to the formation of dialdehyde groups on the corresponding carbon atoms, is a common approach to pectin functionalization [50–52]. The aldehyde groups that are able to react with the amino groups in the Schiff base reaction are attractive for a wide range of biomedical applications [53, 54]. In this study, the content of aldehyde groups in oxidized pectin was 5.70 ± 0.76 mmol/1 g of polymer.

The morphology of the obtained Chit/AF-Pect sponges was evaluated by SEM. SEM images showed the interconnected porous structure of the sponges (Figure 1). The structure of the sponges was dependent on the molecular weight of chitosan. Thus, in the case of high molecular weight chitosan (1,200 kDa), "sponge-like" and "sheet-like" matrices were formed (Figure 1(d)–1(f)). The sponges based on low molecular weight chitosan (30 kDa) were characterized by

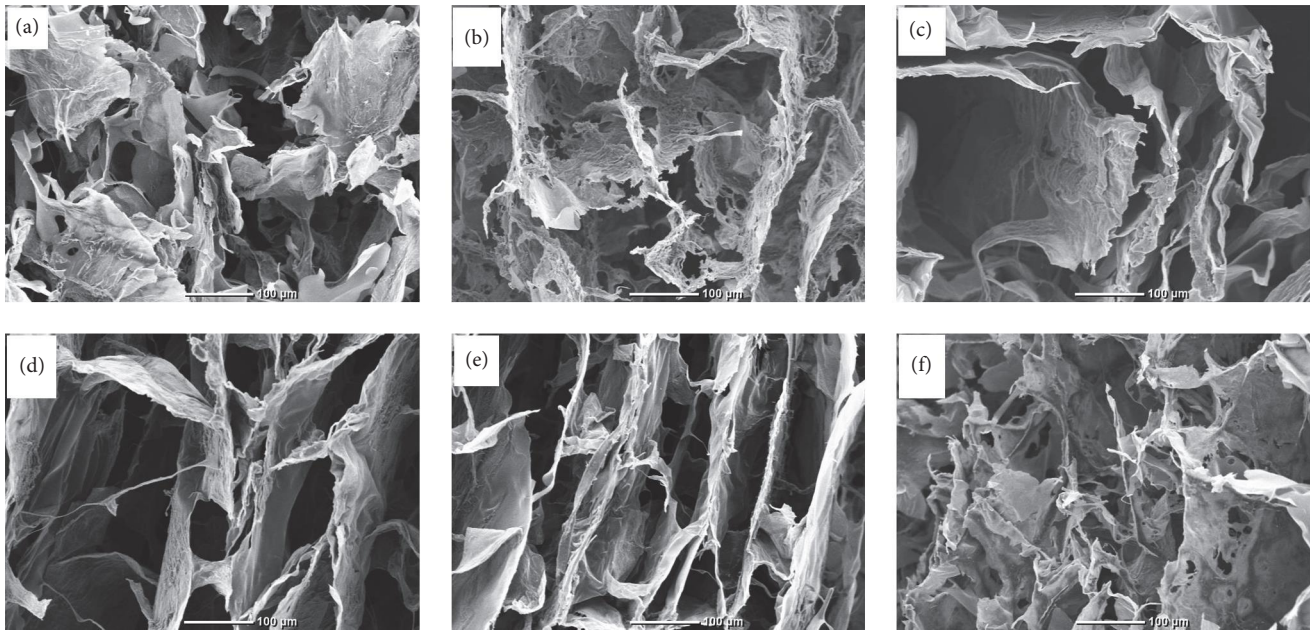

FIGURE 2: Cross-sectional SEM images of Chit/AF-Pect (1 : 1) (a and d), Chit/AF-Pect (2 : 1) (b and e), and Chit/AF-Pect (5 : 1) (c and f) sponges. The molecular weight of chitosan was 30 kDa (a–c) and 1,200 kDa (d–f).

the presence of a thin polymer film on their surface, almost completely covering the internal structure (Figure 1(a)–1(c)). To visualize the "internal" structure of the sponges, cross-sectional SEM images were obtained (Figure 2).

In the case of Chit30, the formation of loose "sponge-like" structures with pores (<10 μm) on the walls was observed (Figures 2(a) and 2(b)). However, for IPEC sponges containing chitosan and AF-Pect in a weight ratio of 5 : 1, no pores were evident on the walls (Figure 2(c)). On the other hand, Chit1200 at the weight ratio of Chit:AF-Pect 1 : 1 and 2 : 1 formed "sheet-like" structures with a distance between sheets of about 50–100 μm (Figures 2(d) and 2(e)). A further increase in the content of chitosan led to the formation of the sponges with a predominantly "sponge-like" structure (Figure 2(f)).

The porosity is a remarkable characteristic of polymeric wound healing materials as it affects the swelling capacity and, therefore, absorption of wound exudate [55, 56]. The high porosity promotes easier penetration of fluid between polymer macromolecules. Furthermore, it ensures better nutrient transport and gas exchange [57, 58]. Some studies have shown that materials with porosities above 90% are appropriate for wound healing applications [59, 60]. The porosity and density of the obtained sponges were about 92.0%–96.0% and 31.0–35.0 mg/cm^3, respectively (Table 1). It was found that the porosity and density of the sponges did not significantly depend on the molecular weight of the chitosan used and the weight ratio of Chit:AF-Pect. The high porosity combined with interconnected porous structure makes Chit/AF-Pect sponges suitable for wound healing applications.

FTIR spectra of Chit30 acetate, original Pect, AF-Pect, and Chit30/AF-Pect (1 : 1) sponge in the range from 4,000 to 400 cm^{-1} are presented in Figure 3. In the spectrum of Chit30 acetate, the characteristic bands at 3,440 (O—H and N—H stretching), 2,923 and 2,886 (C—H symmetric and asymmetric stretching), 1,630 (C═O stretching vibrations, amide I), 1,335 (C—N stretching, amide III), and 1,153 and 898 cm^{-1} (ν_{as} (C—O—C bridge) and C—H bending vibrations of glucopyranose ring) were detected [61, 62]. In addition, three bands at 1,564, 1,411, and 1,384 cm^{-1} assigned to N—H bending vibrations (amide II) and the deformation of—CH_2 and CH_3 groups, respectively, were observed [62, 63].

The FTIR spectrum of original Pect (Figure 3) showed characteristic bands at 3408 (ν (OH)), 2,937 (ν (C—H)), 1,746 (ν (C═O) of ether ($COOCH_3$) or undissociated carboxyl groups), 1,630 (ν_{as} (COO^-)), and 1,334 cm^{-1} (δ (CH)) [8, 64]. Few peaks at 1,200–1,000 cm^{-1} (main maxima: 1,154, 1,110, and 1,014 cm^{-1}) were related to ν (C—O—C) glycosidic bonds, ν (CC) (CO) of the pyranose ring, and ν,δ (C—O—H) [64, 65]. In the spectrum of AF-Pect, some differences with that of Pect were observed. As shown in Figure 3, the intensity of the peak at 1,746 cm^{-1} in the spectrum of original Pect increased in the spectrum of AF-Pect indicating the formation of aldehyde groups, the vibration band of which has overlapped with carboxyl vibration as reported by Chen et al. [52]. Also, an intensification of the band at 1,631 cm^{-1} assigned to asymmetric COO^- stretching vibrations was determined. This may be due to the partial ionization of COOH groups on the polysaccharide backbone [50]. Furthermore, a new band at 1,414 cm^{-1} related to the symmetric COO^- stretching vibrations [64] appeared. In the "finger print region" of the spectrum of AF-Pect, a decrease in the intensity and shift of the maximum of the peak at 1,154 cm^{-1} assigned to ν (C—O—C) glycosidic bonds vibrations were observed. In addition, the shoulder at 954 cm^{-1} (Figure 3) attributed to δ (COH) vibrations appeared as a peak. These alterations confirmed the formation of aldehyde-functionalized pectin following the reaction between pectin and sodium periodate.

Table 1: Characteristics of the obtained Chit/AF-Pect sponges.

Molecular weight of chitosan (kDa)	Weight ratio of Chit:AF-Pect	d (mg/cm^3)	P (%)	Swelling ratio (%)
30	1 : 1	31.0 ± 4.0	94.0 ± 3.0	327 ± 72
	2 : 1	34.0 ± 2.0	96.0 ± 1.0	384 ± 3
	5 : 1	32.0 ± 4.0	94.0 ± 2.0	480 ± 19
1,200	1 : 1	33.0 ± 4.0	92.0 ± 7.0	681 ± 79
	2 : 1	31.0 ± 1.0	92.0 ± 1.0	995 ± 25
	5 : 1	35.0 ± 5.0	96.0 ± 1.0	1,066 ± 55

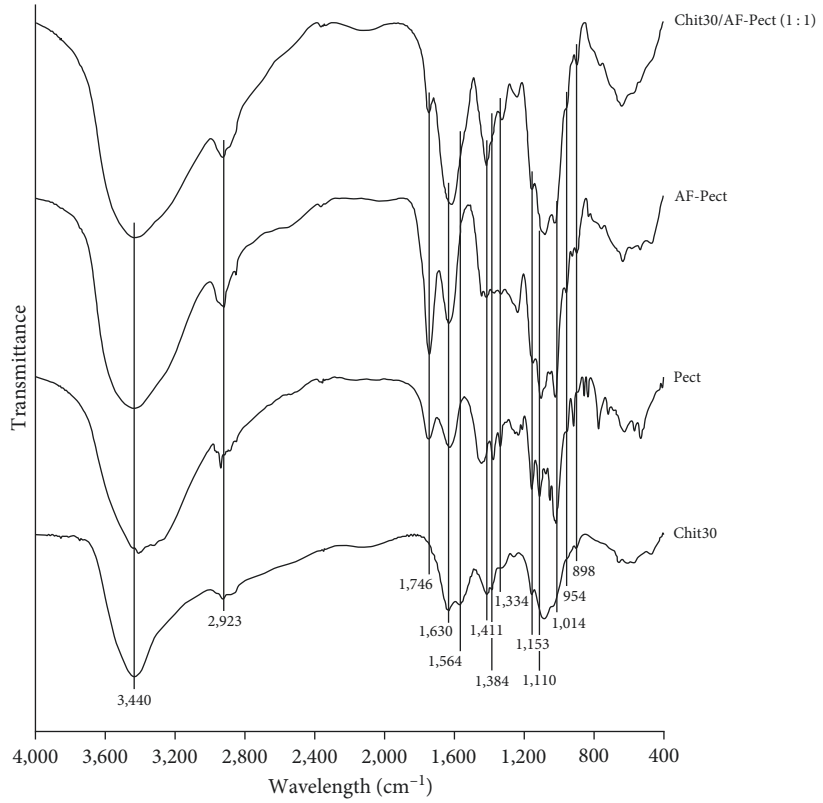

Figure 3: FTIR spectra of Chit30 acetate, Pect, AF-Pect, and Chit30/AF-Pect (1 : 1) sponge.

The FTIR spectrum of Chit30/AF-Pect (1 : 1) sponge showed some changes with those of chitosan and AF-Pect. The main changes occurred in the region between 1,800 and 1,400 cm^{-1} indicating the interaction of carboxyl and aldehyde groups of the oxidized pectin with amino groups of the chitosan [36] and formation of Schiff base between aldehyde and amino functionalities of polysaccharides [66]. Thus, a significant decrease in the intensity of the band at 1,746 cm^{-1} related to ν (C═O) vibration of the nonionized carboxyl groups was observed (Figure 3). In addition, intensification and broadening of the band at 1,631 cm^{-1} were determined. Probably, C═N vibration band has overlapped with carboxylate vibrations [66]. Moreover, the peak at 1,564 cm^1 assigned to N—H bending vibrations in chitosan disappeared, while the intensity of the band at 1,414 cm^{-1} attributed to ν_s (COO$^-$) vibrations in AF-Pect increased. These alterations indicated the successful interaction of aldehyde and carboxyl groups of the oxidized pectin with amino groups of the chitosan and the formation of IPECs.

The thermal stabilities of the samples were monitored using TGA. Thermogravimetric (TG), differential thermogravimetric (DTG), and differential thermal analysis (DTA) curves of original polysaccharides and Chit30/AF-Pect (1 : 1) sponge are shown in Figure 4. On the TG and DTG curves of Chit30 acetate, three consecutive weight loss steps were observed (Figure 4(a)). The first stage was a weight loss of about 9.7% below 120°C, related to physically adsorbed and hydrogen-bonded water release [62, 67]. The second stage (120–360°C) was corresponded to the depolymerization of chitosan and the degradation of pyranose rings [62, 68]. The third stage (up to 600°C) was attributed to the thermo-oxidative process and the destruction of chitosan residues [67, 68]. On the DTA curve, chitosan exhibited an exothermic peak centered at about 285°C and assigned to the thermal

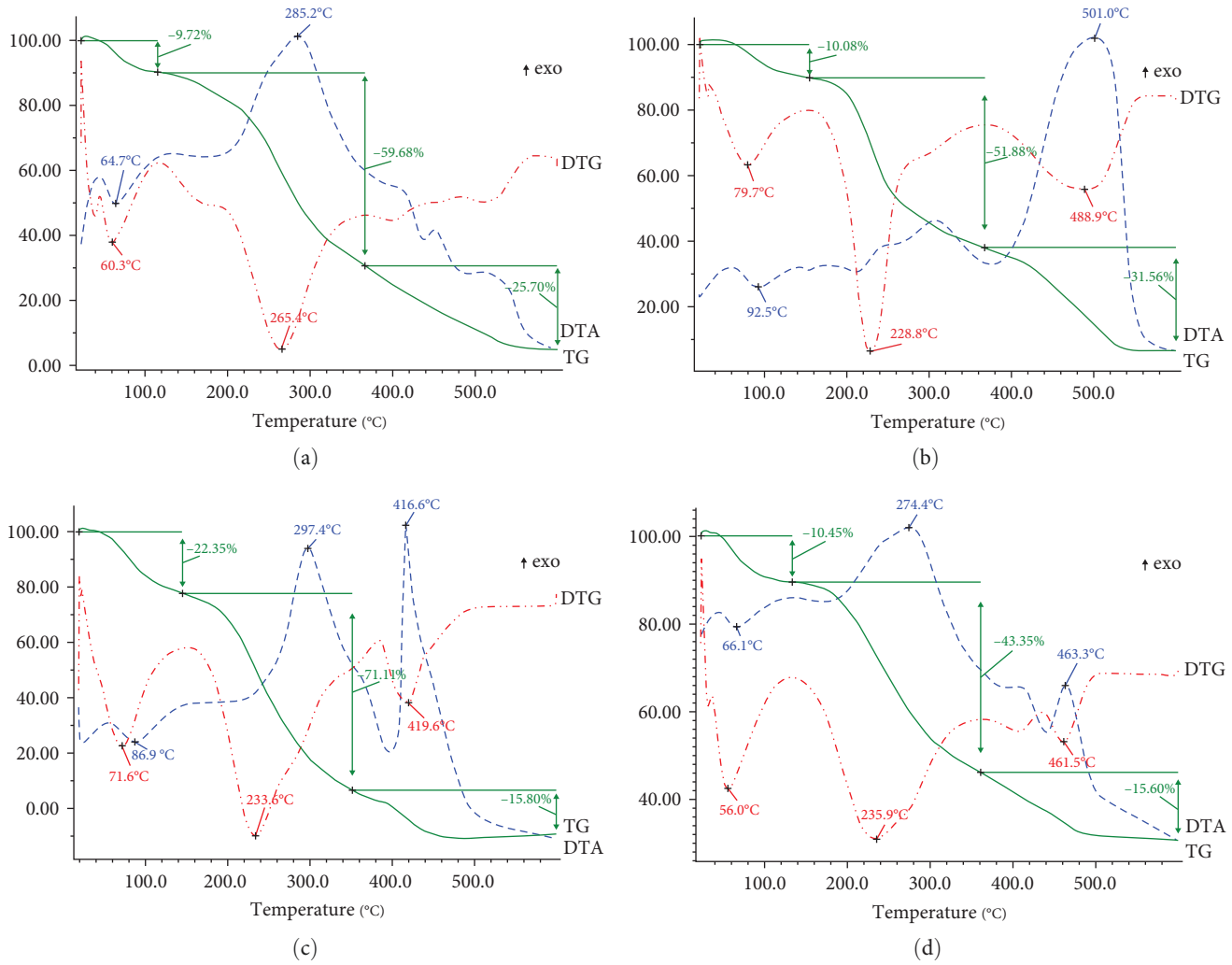

FIGURE 4: TG, DTG, and DTA curves of Chit30 acetate (a), Pect (b), AF-Pect (c), and Chit30/AF-Pect (1 : 1) sponge (d).

decomposition of the polymer [62, 68]. It should be noted that 4.9% of the char residue was found at 600°C.

The thermal stabilities of Pect and AF-Pect were lower compared to Chit30 acetate. TG and DTG curves of Pect and AF-Pect showed three consecutive weight loss steps (Figures 4(b) and 4(c)). The first stage was a weight loss about 10.1% and 22.4% below 160°C, respectively, attributed to water evaporation [69–71]. The second stage (160–360°C) was corresponded to the cracking of bonds or functional groups, structural depolymerization, and chain breaking of the pectin [70–72] and presented the maximum decomposition rate at 228°C and 234°C, respectively. The third stage (up to 600°C) of weight loss (about 31.6% and 15.8%, respectively) could be attributed to the thermo-oxidative process with the formation of volatile degradation products and destruction of pectin residues [73, 74]. After decomposition, 6.5% of the char residue was found at 600°C for Pect, and no char residue was found for AF-Pect.

On the TG and DTG curves of Chit30/AF-Pect (1 : 1) sponge, three consecutive weight loss steps, assigned to water evaporation, depolymerization of polysaccharides, and thermo-oxidative process, were detected (Figure 4(d)). However, the decomposition process began at temperature (T_{onset}) lower than that in the thermograms of the initial components, and the maximum decomposition rate was at about 236°C. Lower thermal stability of the IPEC sponge may be associated with the disturbed organization of IPEC compared to original polysaccharides [75]. Furthermore, 30.6% of the char residue was found at 600°C. Given the amount of char residue after the thermal decomposition of Chit30 and AF-Pect alone and lower T_{onset}, these results confirmed the interaction between —COOH and —CHO groups of oxidized pectin and —NH_2 groups of chitosan and formation of IPECs.

The swelling capacity is a desirable characteristic of polymeric materials for wound repair as it affects the absorption of exudate and the maintenance of a moist wound healing environment [3, 76]. The swelling ratio of porous Chit/AF-Pect sponges depended both on the weight ratio of polysaccharides in the complex and on the molecular weight of chitosan (Table 1). With an increase in the content of chitosan in IPEC, an increase in the swelling ratio by ~1.5–1.6 times was observed: from 327% ± 72% to 480% ± 19% and from 681% ± 79% to 1,066% ± 55% for Chit30 and Chit1200, respectively. Meanwhile, the swelling ratio of sponges based

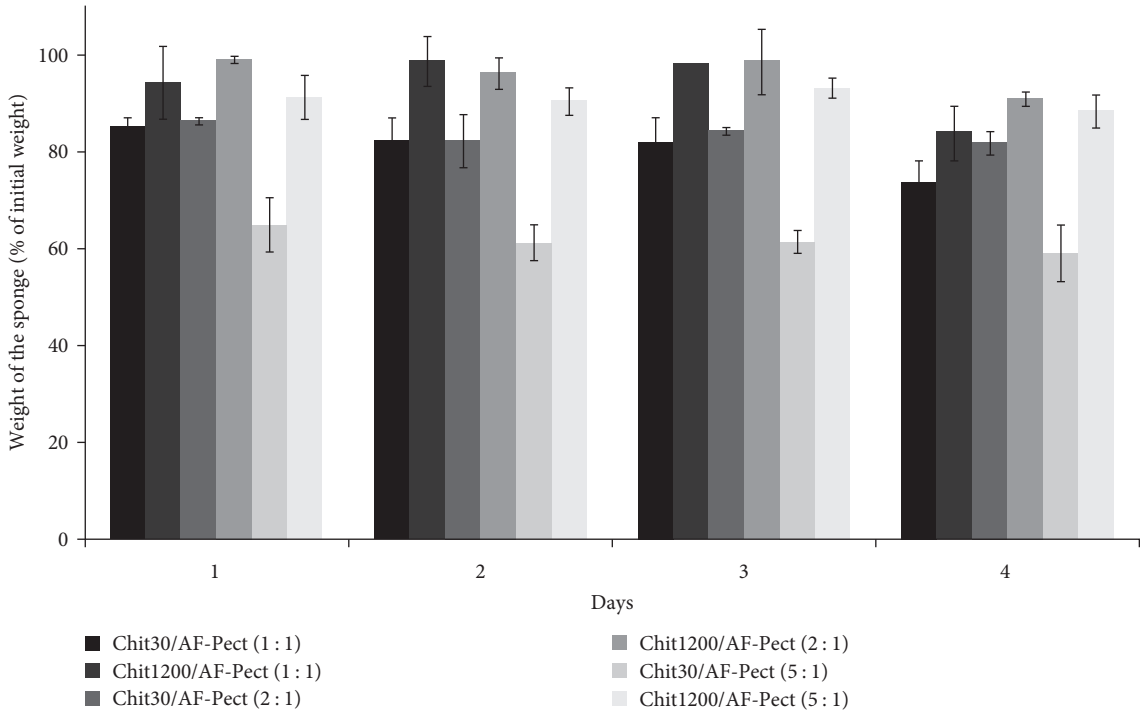

Figure 5: Degradation of Chit/AF-Pect polyelectrolyte complex sponges in DPBS.

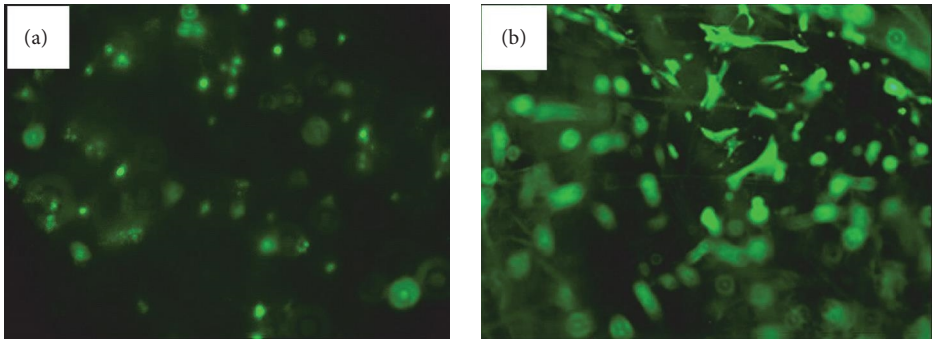

Figure 6: Fluorescent images (green area) of MSCs cultured on Chit30/AF-Pect (1 : 1) (a) and Chit30/AF-Pect (5 : 1) (b) sponges. Magnification ×100.

on Chit1200 was ∼2 times higher compared to matrices containing Chit30 (Table 1). Manatsittipan et al. [77] reported similar effect for polybutylene succinate/chitosan composites: the water absorption increased with increasing molecular weight and content of chitosan.

The degradation of Chit/AF-Pect polyelectrolyte complex sponges was studied in vitro in DPBS (pH 7.0–7.5) at 37°C as a system simulating the isotonic medium of the human body and used in numerous biological applications. After 1 day of immersion, the weight of the Chit30/AF-Pect sponges decreased by around 14%–35%, while the weight of the Chit1200/AF-Pect sponges decreased by 1%–9% (Figure 5). After 4 days, the weight losses of Chit30/AF-Pect and Chit1200/AF-Pect sponges were about 18%–41% and 9%–16%, respectively. The faster degradation of the sponges based on Chit30 may be associated with higher solubility of Chit30 compared to Chit1200 due to its lower molecular weight [78, 79] and increased hydrophilicity arising from the higher degree of deacetylation [80]. Chit30/AF-Pect (5 : 1) sponge was found to be the most degradable: the weight loss was about 41%. This can be explained by the higher content of hydrophilic chitosan in IPEC sponge. It is noteworthy that the sponges retained their integrity after immersion, which indicates the strong interactions between chitosan and AF-Pect.

Further, the cytotoxicity of Chit30/AF-Pect sponges was examined using the FDA/PI cell viability assay as presented in Figure 6. Cytotoxicity is an essential parameter to ensure the sponge's safety for wound healing applications. In this study, Chit30/AF-Pect (1 : 1) and Chit30/AF-Pect (5 : 1) sponges were considered noncytotoxic according to ISO 10993-5 [81], with cell viability values >85% and >70%, respectively. The observed difference in the cytotoxicity of sponges may be related to a different number of free amino groups affecting the bacterial cell wall.

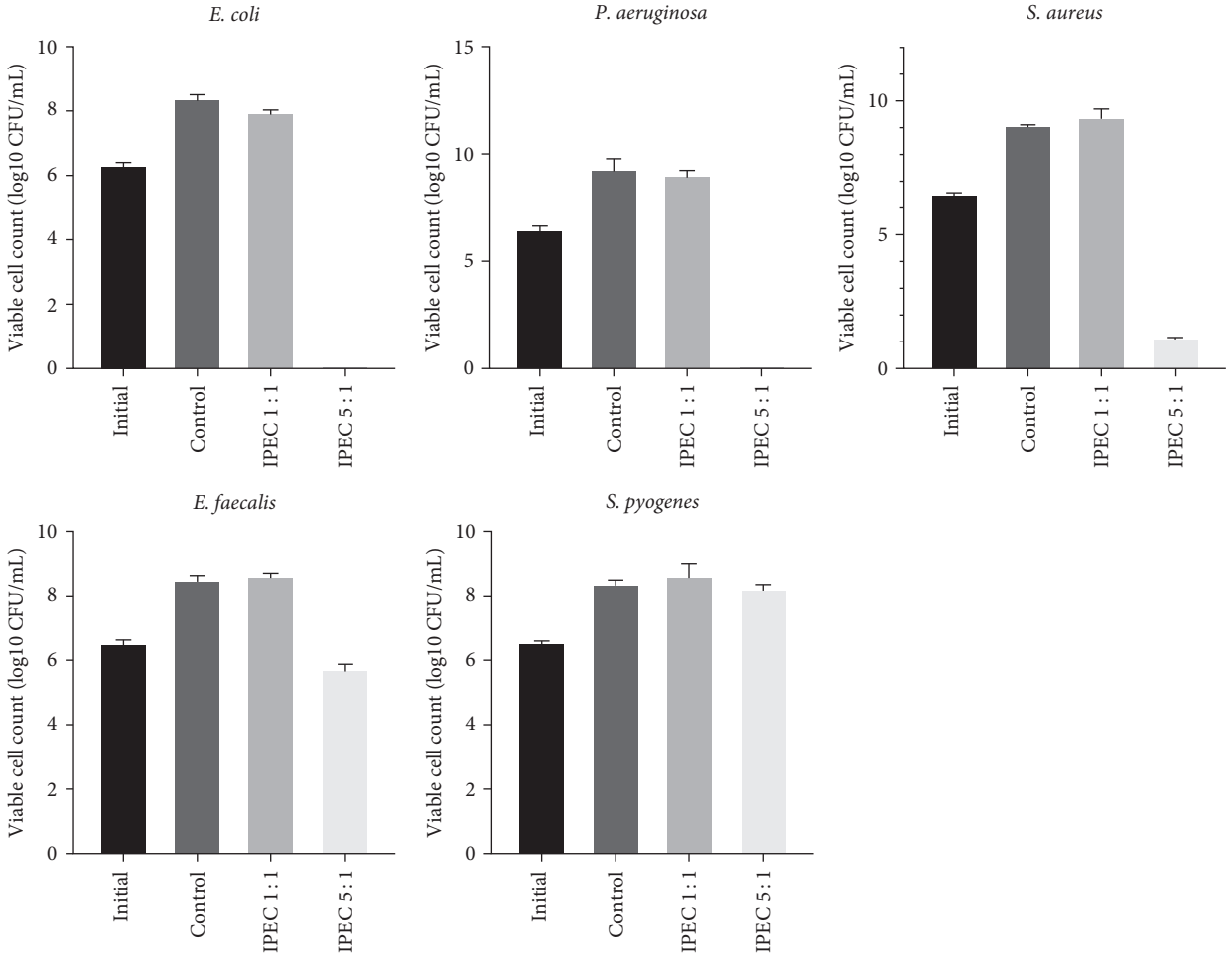

Figure 7: Viable cell count of bacteria after 24-hr incubation in Columbia broth (control) and in the presence of Chit30/AF-Pect (1 : 1) and Chit30/AF-Pect (5 : 1) sponges. Initial–initial concentration of bacterial cells in medium.

Antibacterial activity is an important characteristic of the sponges intended for biomedical applications. Therefore, the antimicrobial properties of Chit30/AF-Pect (1 : 1) and Chit30/AF-Pect (5 : 1) sponges were evaluated against Gram-negative (*E. coli* BIM B-984 G and *P. aeruginosa* BIM B-807 G) and Gram-positive (*E. faecalis* BIM B-1530 G, *S. aureus* BIM B-1841, and *S. pyogenes* BIM B-1529 G) bacteria that cause wound infections. The findings demonstrated that the inhibitory effect of IPEC sponges on bacterial growth varied depending on their chemical composition (Chit:AF-Pect ratio) and bacterial strain (Figure 7). Specifically, Chit30/AF-Pect (1 : 1) sponges were not effective against all bacterial strains tested. In contrast, Chit30/AF-Pect (5 : 1) sponges demonstrated a bactericidal effect against *E. coli* BIM B-984 G, *P. aeruginosa* BIM B-807 G, and *S. aureus* BIM B-1841 strains. Incubation with these IPEC sponges for 24 hr resulted in no detectable viable cells of coliforms and pseudomonads, while the titer of staphylococci decreased to approximately 10 CFU/mL. However, the Chit30/AF-Pect (5 : 1) sponges exhibited only slight antibacterial activity against *E. faecalis* BIM B-1530 G, with a titer reduction of one order of magnitude during the 24-hr incubation period, and no impact was observed on *S. pyogenes* BIM B-1529 G.

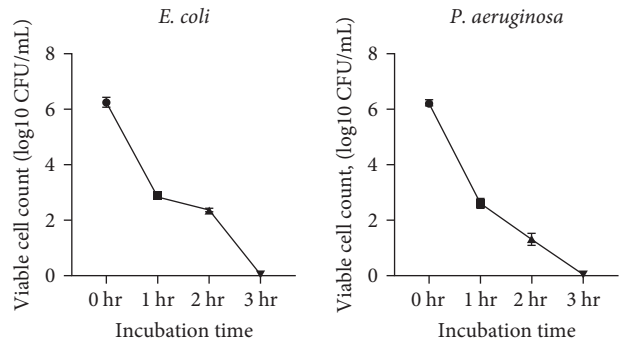

Figure 8: Decrease in viable cell count of *E. coli* BIM B-984 G and *P. aeruginosa* BIM B-807 G upon incubation with Chit30/AF-Pect (5 : 1) sponges.

The investigation of the decrease rate in the viable cell count of *E. coli* BIM B-984 G and *P. aeruginosa* BIM B-807 G upon incubation with Chit30/AF-Pect (5 : 1) sponges showed a significant decrease of four orders of magnitude after 1 hr of exposure, with complete elimination of viable cells after 3 hr for both strains (Figure 8).

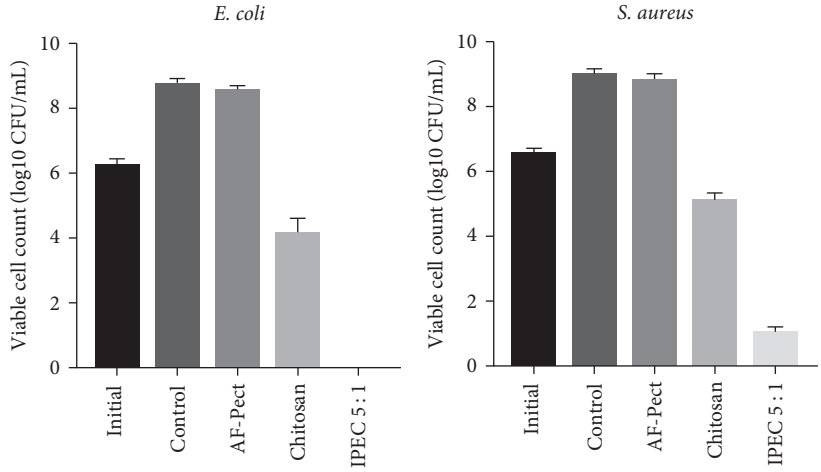

Figure 9: Viable cell count of *E. coli* BIM B-984 G and *P. aeruginosa* BIM B-807 G after 24-hr incubation in Columbia broth (control) and in the presence of AF-Pect, Chit30, and Chit30/AF-Pect (5 : 1) sponges. Initial–initial concentration of bacterial cells in medium.

The results of the comparative analysis indicated that Chit30/AF-Pect (5 : 1) sponges exhibited greater antibacterial activity against both Gram-negative (*E. coli* BIM B-984 G) and Gram-positive (*S. aureus* BIM B-1841) bacteria than pure AF-Pect and Chit30 sponges (Figure 9). During the 24-hr incubation period, the AF-Pect sponges did not reduce the number of viable cells of coliforms and staphylococci. On the contrary, bacterial cultures were observed to grow in the presence of pure AF-Pect, similar to the control. Chit30 sponges decreased the titer of *E. coli* BIM B-984 G and *S. aureus* BIM B-1841 by two and one order of magnitude, respectively, compared to the initial titer (Figure 9). However, incubation with Chit30/AF-Pect (5 : 1) sponges resulted in a five-order of magnitude decrease in the number of viable staphylococci cells (to ∼10 CFU/mL), and no viable cells of *E. coli* BIM B-984 G were detected.

The mechanism of antimicrobial action of chitosan and its derivatives is not been fully understood. However, there is clear evidence that these compounds interact with the cell membrane of microorganisms at a molecular level. Therefore, the main factor contributing to the antibacterial activity of chitosan and its derivatives is the electrostatic interaction between the positively charged amino groups of chitosan and the anionic groups present on the bacterial cell surface. This interaction leads to alterations in the cell wall of Gram-positive bacteria or the outer membrane of Gram-negative bacteria, which in turn causes disruptions in cytoplasmic membrane permeability. As a result, essential constituents such as enzymes, nucleotides, and ions are lost, ultimately leading to bacterial cell death [11, 82, 83]. Moreover, the antibacterial activity of chitosan and its derivatives is significantly influenced by the degree of deacetylation, which directly affects the positive charge density. It is believed that a higher positive charge density leads to stronger electrostatic interaction with bacterial cells [84]. Therefore, we hypothesized that the increased antibacterial effect of Chit30/AF-Pect (5 : 1) sponges compared to original polymers may be due to the formation of Schiff bases with imine groups (—RC═N—) from the interaction between chitosan's amino groups and oxidized pectin's aldehyde groups that enhances the positive charge of chitosan [85, 86]. Similar results were reported for interpolyelectrolyte complexes of poly(acrylic acid)–chitosan [87], chitosan–alginate, chitosan–*κ*-carrageenan [88], and chitosan-oxidized pectin [51]. These polyelectrolyte complexes exhibited higher antibacterial activity against *P. aeruginosa*, *P. oleovorans*, and *E. coli*, *S. aureus*, and *B. subtilis* and *S. aureus*, respectively, than the original chitosan.

The variations in antibacterial effect of IPEC sponges against the tested bacterial strains may be due to their individual susceptibility, which is dependent on particular structural and functional traits of the cells. Thus, IPEC sponges were more effective in inhibiting the growth of Gram-negative bacteria (*E. coli* BIM B-984 G and *P. aeruginosa* BIM B-807 G) compared to Gram-positive bacteria (*E. faecalis* BIM B-1530 G, *S. aureus* BIM B-1841, and *S. pyogenes* BIM B-1529 G). These results are consistent with the findings of other research groups, which suggest that Gram-negative bacteria may be more susceptible to chitosan and its derivatives due to the higher negative charge of their cell surfaces [83, 84].

The study found that Chit30/AF-Pect (5 : 1) sponges exhibit strong antibacterial activity against *E. coli* BIM B-984 G, *P. aeruginosa* BIM B-807 G, and *S. aureus* BIM B-1841, representing the major bacterial species causing wound infections, signifying the potential of using these polyelectrolyte complex sponges for developing antibacterial wound dressings.

4. Conclusions

In the present study, porous materials based on polyelectrolyte complexes of chitosan and oxidized pectin were obtained by freeze-drying technique. Pectin functionalization with dialdehyde groups was confirmed by FTIR spectroscopy and TGA. The study demonstrated increasing molecular weight and content of chitosan led to a higher swelling capacity of the formed IPEC sponges. Chit1200/AF-Pect sponges also showed lower degradability compared to the Chit30/AF-Pect ones. Additionally, Chit30/AF-Pect sponges were found to be noncytotoxic, with cell viability values >70%. Furthermore,

the obtained Chit30/AF-Pect (5 : 1) sponges exhibited antibacterial activity against *E. coli* BIM B-984 G, *P. aeruginosa* BIM B-807 G, and *S. aureus* BIM B-1841. Given the good swelling capacity, noncytotoxicity, and strong antibacterial properties, the obtained Chit30/AF-Pect (5 : 1) sponges can be promising as materials for developing antibacterial wound dressings for wound healing applications.

Data Availability

The datasets generated during and/or analyzed during the current study are available from the corresponding author on reasonable request.

Conflicts of Interest

The authors declare that they have no conflicts of interest.

Authors' Contributions

Aliaksandr Kraskouski, Viktoryia Kulikouskaya, and Anastasiya Sidarenka are responsible for the conceptualization of the study; Aliaksandr Kraskouski, Maksim Mashkin, Viktoryia Savich, and Sergei Pinchuk are responsible for formal analysis and investigation; Aliaksandr Kraskouski is responsible for writing—original draft preparation; Viktoryia Kulikouskaya, Anastasiya Sidarenka, and Ruibin Li are responsible for writing—review and editing; and Viktoryia Kulikouskaya, Anastasiya Sidarenka, and Ruibin Li are responsible for supervision.

Acknowledgments

This study was financially supported by the Belarusian Republican Foundation for Fundamental Research (grant no. M21UZBG-021).

References

[1] C. Hua, T. Urbina, R. Bosc et al., "Necrotising soft-tissue infections," *The Lancet Infectious Diseases*, vol. 23, no. 3, pp. e81–e94, 2023.

[2] F. Nawijn, D. P. J. Smeeing, R. M. Houwert, L. P. H. Leenen, and F. Hietbrink, "Time is of the essence when treating necrotizing soft tissue infections: a systematic review and meta-analysis," *World Journal of Emergency Surgery*, vol. 15, no. 1, 2020.

[3] J. S. Boateng, K. H. Matthews, H. N. E. Stevens, and G. M. Eccleston, "Wound healing dressings and drug delivery systems: a review," *Journal of Pharmaceutical Sciences*, vol. 97, no. 8, pp. 2892–2923, 2008.

[4] Z. A. Khan, S. Jamil, A. Akhtar, M. M. Bashir, and M. Yar, "Chitosan based hybrid materials used for wound healing application—a short review," *International Journal of Polymeric Materials and Polymeric Biomaterials*, vol. 69, no. 7, pp. 419–436, 2020.

[5] D. M. L. Ribeiro, A. R. C. Júnior, G. H. R. V. de Macedo et al., "Polysaccharide-based formulations for healing of skin-related wound infections: lessons from animal models and clinical trials," *Biomolecules*, vol. 10, no. 1, Article ID 63, 2020.

[6] M. Tavakoli, S. Labbaf, M. Mirhaj, S. Salehi, A. M. Seifalian, and M. Firuzeh, "Natural polymers in wound healing: from academic studies to commercial products," *Journal of Applied Polymer Science*, vol. 140, no. 22, 2023.

[7] T. G. Sahana and P. D. Rekha, "Biopolymers: applications in wound healing and skin tissue engineering," *Molecular Biology Reports*, vol. 45, no. 6, pp. 2857–2867, 2018.

[8] V. Kulikouskaya, A. Kraskouski, K. Hileuskaya, A. Zhura, S. Tratsyak, and V. Agabekov, "Fabrication and characterization of pectin-based three-dimensional porous scaffolds suitable for treatment of peritoneal adhesions," *Journal of Biomedical Materials Research Part A*, vol. 107, no. 8, pp. 1814–1823, 2019.

[9] A. Sidarenka, A. Kraskouski, V. Savich et al., "Design of sponge-like chitosan wound dressing with immobilized bacteriophages for promoting healing of bacterially infected wounds," *Journal of Polymers and the Environment*, 2024.

[10] G. P. Rajalekshmy, L. L. Devi, J. Joseph, and M. R. Rekha, "An overview on the potential biomedical applications of polysaccharides," in *Functional Polysaccharides for Biomedical Applications*, S. Maiti and S. Jana, Eds., pp. 33–94, Woodhead Publishing, 2019.

[11] A. Verlee, S. Mincke, and C. V. Stevens, "Recent developments in antibacterial and antifungal chitosan and its derivatives," *Carbohydrate Polymers*, vol. 164, pp. 268–283, 2017.

[12] D. Meng, B. Garba, Y. Ren et al., "Antifungal activity of chitosan against *Aspergillus ochraceus* and its possible mechanisms of action," *International Journal of Biological Macromolecules*, vol. 158, pp. 1063–1070, 2020.

[13] J. Li and S. Zhuang, "Antibacterial activity of chitosan and its derivatives and their interaction mechanism with bacteria: current state and perspectives," *European Polymer Journal*, vol. 138, Article ID 109984, 2020.

[14] M. N. Sundaram, U. Mony, and R. Jayakumar, "Chitin and chitosan as hemostatic agents," in *Encyclopedia of Polymer Science and Technology*, pp. 1–12, John Wiley & Sons, Inc, Hoboken, NJ, USA, 2016.

[15] Z. Liu, Y. Xu, H. Su et al., "Chitosan-based hemostatic sponges as new generation hemostatic materials for uncontrolled bleeding emergency: modification, composition, and applications," *Carbohydrate Polymers*, vol. 311, Article ID 120780, 2023.

[16] E. M. A. Hejjaji, A. M. Smith, and G. A. Morris, "Evaluation of the mucoadhesive properties of chitosan nanoparticles prepared using different chitosan to tripolyphosphate (CS: TPP) ratios," *International Journal of Biological Macromolecules*, vol. 120, pp. 1610–1617, 2018.

[17] H. Hamedi, S. Moradi, S. M. Hudson, A. E. Tonelli, and M. W. King, "Chitosan based bioadhesives for biomedical applications: a review," *Carbohydrate Polymers*, vol. 282, Article ID 119100, 2022.

[18] I. Aranaz, A. R. Alcántara, M. C. Civera et al., "Chitosan: an overview of its properties and applications," *Polymers*, vol. 13, no. 19, Article ID 3256, 2021.

[19] M. M. Islam, M. Shahruzzaman, S. Biswas, M. N. Sakib, and T. U. Rashid, "Chitosan based bioactive materials in tissue engineering applications—a review," *Bioactive Materials*, vol. 5, no. 1, pp. 164–183, 2020.

[20] H. Liu, C. Wang, C. Li et al., "A functional chitosan-based hydrogel as a wound dressing and drug delivery system in the treatment of wound healing," *RSC Advances*, vol. 8, no. 14, pp. 7533–7549, 2018.

[21] B. Tian, S. Hua, and J. Liu, "Multi-functional chitosan-based nanoparticles for drug delivery: recent advanced insight into

cancer therapy," *Carbohydrate Polymers*, vol. 315, Article ID 120972, 2023.

[22] P. Feng, Y. Luo, C. Ke et al., "Chitosan-based functional materials for skin wound repair: mechanisms and applications," *Frontiers in Bioengineering and Biotechnology*, vol. 9, 2021.

[23] M. Zou, X. Hu, Y. Wang, J. Wang, F. Tang, and Y. Liu, "Structural characterization and anti-inflammatory activity of a pectin polysaccharide HBHP-3 from *Houttuynia cordata*," *International Journal of Biological Macromolecules*, vol. 210, pp. 161–171, 2022.

[24] N. Thirawong, J. Nunthanid, S. Puttipipatkhachorn, and P. Sriamornsak, "Mucoadhesive properties of various pectins on gastrointestinal mucosa: an in vitro evaluation using texture analyzer," *European Journal of Pharmaceutics and Biopharmaceutics*, vol. 67, no. 1, pp. 132–140, 2007.

[25] R. Ciriminna, A. Fidalgo, F. Meneguzzo et al., "Pectin: a long-neglected broad-spectrum antibacterial," *ChemMedChem*, vol. 15, no. 23, pp. 2228–2235, 2020.

[26] M. R. Harsha, S. V. Chandra Prakash, and S. M. Dharmesh, "Modified pectic polysaccharide from turmeric (*Curcuma longa*): a potent dietary component against gastric ulcer," *Carbohydrate Polymers*, vol. 138, pp. 143–155, 2016.

[27] H. Ding and S. W. Cui, *Pectin Bioactivity, in: Pectin: Technological and Physiological Properties*, pp. 165–188, Springer, Cham, 2020.

[28] A. Noreen, Z.-H. Nazli, J. Akram et al., "Pectins functionalized biomaterials; a new viable approach for biomedical applications: a review," *International Journal of Biological Macromolecules*, vol. 101, pp. 254–272, 2017.

[29] R. Eivazzadeh-Keihan, E. B. Noruzi, H. A. M. Aliabadi et al., "Recent advances on biomedical applications of pectin-containing biomaterials," *International Journal of Biological Macromolecules*, vol. 217, pp. 1–18, 2022.

[30] E. G. Andriotis, G. K. Eleftheriadis, C. Karavasili, and D. G. Fatouros, "Development of bio-active patches based on pectin for the treatment of ulcers and wounds using 3D-bioprinting technology," *Pharmaceutics*, vol. 12, no. 1, Article ID 56, 2020.

[31] S. Vasiliu, S. Racovita, M. Popa, L. Ochiuz, and C. A. Peptu, "Chitosan-based polyelectrolyte complex hydrogels for biomedical applications," in *Cellulose-Based Superabsorbent Hydrogels*, M. Mondal, Ed., Polymers and Polymeric Composites: A Reference Series (POPOC), pp. 1–31, Springer, Cham, Switzerland, 2019.

[32] S. Khorshidi, A. Karkhaneh, S. Bonakdar, and M. Omidian, "High-strength functionalized pectin/fibroin hydrogel with tunable properties: a structure-property relationship study," *Journal of Applied Polymer Science*, vol. 137, no. 28, Article ID 48859, 2020.

[33] A. D. Kulkarni, Y. H. Vanjari, K. H. Sancheti et al., "Polyelectrolyte complexes: mechanisms, critical experimental aspects, and applications," *Artificial Cells, Nanomedicine, and Biotechnology*, vol. 44, no. 7, pp. 1615–1625, 2016.

[34] V. S. Meka, M. K. G. Sing, M. R. Pichika, S. R. Nali, V. R. M. Kolapalli, and P. Kesharwani, "A comprehensive review on polyelectrolyte complexes," *Drug Discovery Today*, vol. 22, no. 11, pp. 1697–1706, 2017.

[35] D. Kulig, A. Zimoch-Korzycka, A. Jarmoluk, and K. Marycz, "Study on alginate-chitosan complex formed with different polymers ratio," *Polymers*, vol. 8, no. 5, Article ID 167, 2016.

[36] V. B. V. Maciel, C. M. P. Yoshida, and T. T. Franco, "Chitosan/pectin polyelectrolyte complex as a pH indicator," *Carbohydrate Polymers*, vol. 132, pp. 537–545, 2015.

[37] N. Barroso, O. Guaresti, L. Pérez-Álvarez, L. Ruiz-Rubio, N. Gabilondo, and J. L. Vilas-Vilela, "Self-healable hyaluronic acid/chitosan polyelectrolyte complex hydrogels and multilayers," *European Polymer Journal*, vol. 120, Article ID 109268, 2019.

[38] D. C. M. Ferreira, S. O. Ferreira, E. S. de Alvarenga, N. F. F. Soares, J. S. R. Coimbra, and E. B. de Oliveira, "Polyelectrolyte complexes (PECs) obtained from chitosan and carboxymethylcellulose: a physicochemical and microstructural study," *Carbohydrate Polymer Technologies and Applications*, vol. 3, Article ID 100197, 2022.

[39] N. G. Voron'ko, S. R. Derkach, Y. A. Kuchina, and N. I. Sokolan, "The chitosan-gelatin (bio)polyelectrolyte complexes formation in an acidic medium," *Carbohydrate Polymers*, vol. 138, pp. 265–272, 2016.

[40] Y. Luo and Q. Wang, "Recent development of chitosan-based polyelectrolyte complexes with natural polysaccharides for drug delivery," *International Journal of Biological Macromolecules*, vol. 64, pp. 353–367, 2014.

[41] J. H. Hamman, "Chitosan based polyelectrolyte complexes as potential carrier materials in drug delivery systems," *Marine Drugs*, vol. 8, no. 4, pp. 1305–1322, 2010.

[42] N. V. Dubashynskaya, E. R. Gasilova, and Y. A. Skorik, "Nano-sized fucoidan interpolyelectrolyte complexes: recent advances in design and prospects for biomedical applications," *International Journal of Molecular Sciences*, vol. 24, no. 3, Article ID 2615, 2023.

[43] C. Ceccaldi, R. Bushkalova, C. Alfarano et al., "Evaluation of polyelectrolyte complex-based scaffolds for mesenchymal stem cell therapy in cardiac ischemia treatment," *Acta Biomaterialia*, vol. 10, no. 2, pp. 901–911, 2014.

[44] Q. Cui, D. J. Bell, S. B. Rauer, and M. Wessling, "Wet-spinning of biocompatible core-shell polyelectrolyte complex fibers for tissue engineering," *Advanced Materials Interfaces*, vol. 7, no. 23, 2020.

[45] M. Shu, S. Long, Y. Huang, D. Li, H. Li, and X. Li, "High strength and antibacterial polyelectrolyte complex CS/HS hydrogel films for wound healing," *Soft Matter*, vol. 15, no. 38, pp. 7686–7694, 2019.

[46] S. Sharma, K. L. Swetha, and A. Roy, "Chitosan–chondroitin sulfate based polyelectrolyte complex for effective management of chronic wounds," *International Journal of Biological Macromolecules*, vol. 132, pp. 97–108, 2019.

[47] M. Patenaude and T. Hoare, "Injectable, mixed natural-synthetic polymer hydrogels with modular properties," *Biomacromolecules*, vol. 13, no. 2, pp. 369–378, 2012.

[48] V. Kulikouskaya, M. Lazouskaya, and V. Agabekov, "Fabrication and physicochemical properties of pectin/chitosan scaffolds," *Engineering of Biomaterials*, vol. 21, pp. 2–7, 2018.

[49] K. Hileuskaya, B. Kakasi, V. Kulikouskaya et al., "Contact guidance of mesenchymal stem cells by flagellin-modified substrates: aspects of cell-surface interaction from the point of view of liquid crystal theory," *Colloids and Surfaces A: Physicochemical and Engineering Aspects*, vol. 663, Article ID 131113, 2023.

[50] B. Gupta, M. Tummalapalli, B. L. Deopura, and M. S. Alam, "Functionalization of pectin by periodate oxidation," *Carbohydrate Polymers*, vol. 98, no. 1, pp. 1160–1165, 2013.

[51] A. Chetouani, N. Follain, S. Marais et al., "Physicochemical properties and biological activities of novel blend films using oxidized pectin/chitosan," *International Journal of Biological Macromolecules*, vol. 97, pp. 348–356, 2017.

[52] S. Chen, S. Cui, H. Zhang et al., "Cross-linked pectin nanofibers with enhanced cell adhesion," *Biomacromolecules*, vol. 19, no. 2, pp. 490–498, 2018.

[53] R. M. A. Domingues, M. Silva, P. Gershovich et al., "Development of injectable hyaluronic acid/cellulose nanocrystals bionanocomposite hydrogels for tissue engineering applications," *Bioconjugate Chemistry*, vol. 26, no. 8, pp. 1571–1581, 2015.

[54] M. Zhang, X. Qiao, W. Han, T. Jiang, F. Liu, and X. Zhao, "Alginate-chitosan oligosaccharide-ZnO composite hydrogel for accelerating wound healing," *Carbohydrate Polymers*, vol. 266, Article ID 118100, 2021.

[55] P. Deng, W. Jin, Z. Liu, M. Gao, and J. Zhou, "Novel multifunctional adenine-modified chitosan dressings for promoting wound healing," *Carbohydrate Polymers*, vol. 260, Article ID 117767, 2021.

[56] A. Nepal, H. D. N. Tran, N.-T. Nguyen, and H. T. Ta, "Advances in haemostatic sponges: characteristics and the underlying mechanisms for rapid haemostasis," *Bioactive Materials*, vol. 27, pp. 231–256, 2023.

[57] Q. L. Loh and C. Choong, "Three-dimensional scaffolds for tissue engineering applications: role of porosity and pore size," *Tissue Engineering Part B: Reviews*, vol. 19, no. 6, pp. 485–502, 2013.

[58] Lá L. Lima, T. B. Taketa, M. M. Beppu, I. M.de O. Sousa, M. A. Foglio, and Â. M. Moraes, "Coated electrospun bioactive wound dressings: mechanical properties and ability to control lesion microenvironment," *Materials Science & Engineering. C, Materials for Biological Applications*, vol. 100, pp. 493–504, 2019.

[59] T. M. Freyman, I. V. Yannas, and L. J. Gibson, "Cellular materials as porous scaffolds for tissue engineering," *Progress in Materials Science*, vol. 46, no. 3-4, pp. 273–282, 2001.

[60] S. P. Miguel, M. P. Ribeiro, P. Coutinho, and I. J. Correia, "Electrospun polycaprolactone/aloe vera_chitosan nanofibrous asymmetric membranes aimed for wound healing applications," *Polymers*, vol. 9, no. 12, Article ID 183, 2017.

[61] V. Nikalaichuk, K. Hileuskaya, A. Kraskouski et al., "Chitosan-hydroxycinnamic acid conjugates: synthesis, photostability and phytotoxicity to seed germination of barley," *Journal of Applied Polymer Science*, vol. 139, no. 14, Article ID 51884, 2022.

[62] A. Kraskouski, K. Hileuskaya, V. Nikalaichuk et al., "Chitosan-based Maillard self-reaction products:formation, characterization, antioxidant and antimicrobial potential," *Carbohydrate Polymer Technologies and Applications*, vol. 4, Article ID 100257, 2022.

[63] H. Yang, Y. Zhang, F. Zhou et al., "Preparation, bioactivities and applications in food industry of chitosan-based Maillard products: a review," *Molecules*, vol. 26, no. 1, Article ID 166, 2021.

[64] L. C. Bichara, P. E. Alvarez, M. V. Fiori Bimbi, H. Vaca, C. Gervasi, and S. A. Brandán, "Structural and spectroscopic study of a pectin isolated from citrus peel by using FTIR and FT-Raman spectra and DFT calculations," *Infrared Physics & Technology*, vol. 76, pp. 315–327, 2016.

[65] A. Kraskouski, K. Hileuskaya, A. Ladutska et al., "Multifunctional biocompatible films based on pectin-Ag nanocomposites and PVA: design, characterization and antimicrobial potential," *Journal of Applied Polymer Science*, vol. 139, no. 42, 2022.

[66] L. Fan, Y. Sun, W. Xie, H. Zheng, and S. Liu, "Oxidized pectin cross-linked carboxymethyl chitosan: a new class of hydrogels," *Journal of Biomaterials Science, Polymer Edition*, vol. 23, no. 16, pp. 2119–2132, 2012.

[67] H. Moussout, H. Ahlafi, M. Aazza, and M. Bourakhouadar, "Kinetics and mechanism of the thermal degradation of biopolymers chitin and chitosan using thermogravimetric analysis," *Polymer Degradation and Stability*, vol. 130, pp. 1–9, 2016.

[68] J. Zawadzki and H. Kaczmarek, "Thermal treatment of chitosan in various conditions," *Carbohydrate Polymers*, vol. 80, no. 2, pp. 394–400, 2010.

[69] A. M. M. Combo, M. Aguedo, N. Quiévy et al., "Characterization of sugar beet pectic-derived oligosaccharides obtained by enzymatic hydrolysis," *International Journal of Biological Macromolecules*, vol. 52, pp. 148–156, 2013.

[70] J. Aburto, M. Moran, A. Galano, and E. Torres-García, "Non-isothermal pyrolysis of pectin: a thermochemical and kinetic approach," *Journal of Analytical and Applied Pyrolysis*, vol. 112, pp. 94–104, 2015.

[71] B. A. Balik, S. Argin, J. M. Lagaron, and S. Torres-Giner, "Preparation and characterization of electrospun pectin-based films and their application in sustainable aroma barrier multilayer packaging," *Applied Sciences*, vol. 9, no. 23, Article ID 5136, 2019.

[72] W. Wang, X. Ma, P. Jiang et al., "Characterization of pectin from grapefruit peel: a comparison of ultrasound-assisted and conventional heating extractions," *Food Hydrocolloids*, vol. 61, pp. 730–739, 2016.

[73] S. Zhou, Y. Xu, C. Wang, and Z. Tian, "Pyrolysis behavior of pectin under the conditions that simulate cigarette smoking," *Journal of Analytical and Applied Pyrolysis*, vol. 91, no. 1, pp. 232–240, 2011.

[74] E. Calce, V. Bugatti, V. Vittoria, and S. De Luca, "Solvent-free synthesis of modified pectin compounds promoted by microwave irradiation," *Molecules*, vol. 17, no. 10, pp. 12234–12242, 2012.

[75] J. Kowalonek, "Studies of chitosan/pectin complexes exposed to UV radiation," *International Journal of Biological Macromolecules*, vol. 103, pp. 515–524, 2017.

[76] G. Lan, S. Zhu, D. Chen, H. Zhang, L. Zou, and Y. Zeng, "Highly adhesive antibacterial bioactive composite hydrogels with controllable flexibility and swelling as wound dressing for full-thickness skin healing," *Frontiers in Bioengineering and Biotechnology*, vol. 9, 2021.

[77] S. Manatsittipan, K. Kuttiyawong, K. Ito, and S. Tiptipakorn, "Effects of molecular weight of chitosan on the biodegradability and thermal properties of polybutylene succinate/chitosan composites," *Key Engineering Materials*, vol. 775, pp. 26–31, 2018.

[78] N. Kubota and Y. Eguchi, "Facile preparation of water-soluble N-acetylated chitosan and molecular weight dependence of its water-solubility," *Polymer Journal*, vol. 29, no. 2, pp. 123–127, 1997.

[79] S. Suryani, A. Y. Chaerunisaa, I. M. Joni et al., "Production of low molecular weight chitosan using a combination of weak acid and ultrasonication methods," *Polymers*, vol. 14, no. 16, Article ID 3417, 2022.

[80] C. K. S. Pillai, W. Paul, and C. P. Sharma, "Chitin and chitosan polymers: chemistry, solubility and fiber formation," *Progress in Polymer Science*, vol. 34, no. 7, pp. 641–678, 2009.

[81] ISO 10993-5, *Biological Evaluation of Medical Devices—Part 5: Tests for in Vitro Cytotoxicity*, International Organization for Standardization., 2009.

[82] P. Sahariah and M. Másson, "Antimicrobial chitosan and chitosan derivatives: a review of the structure-activity relationship," *Biomacromolecules*, vol. 18, no. 11, pp. 3846–3868, 2017.

[83] L. G. Confederat, C. G. Tuchilus, M. Dragan, M. Sha'at, and O. M. Dragostin, "Preparation and antimicrobial activity of chitosan and its derivatives: a concise review," *Molecules*, vol. 26, no. 12, Article ID 3694, 2021.

[84] M. Kong, X. G. Chen, K. Xing, and H. J. Park, "Antimicrobial properties of chitosan and mode of action: a state of the art review," *International Journal of Food Microbiology*, vol. 144, no. 1, pp. 51–63, 2010.

[85] T. M. Tamer, M. A. Hassan, A. M. Omer et al., "Synthesis, characterization and antimicrobial evaluation of two aromatic chitosan Schiff base derivatives," *Process Biochemistry*, vol. 51, no. 10, pp. 1721–1730, 2016.

[86] M. A. Hassan, A. M. Omer, E. Abbas, W. M. A. Baset, and T. M. Tamer, "Preparation, physicochemical characterization and antimicrobial activities of novel two phenolic chitosan Schiff base derivatives," *Scientific Reports*, vol. 8, no. 1, 2018.

[87] H. Ortega-Ortiz, B. Gutiérrez-Rodríguez, G. Cadenas-Pliego, and L. I. Jimenez, "Antibacterial activity of chitosan and the interpolyelectrolyte complexes of poly(acrylic acid)-chitosan," *Brazilian Archives of Biology and Technology*, vol. 53, no. 3, pp. 623–628, 2010.

[88] N. Ismillayli, I. G. A. S. Andayani, R. Honiar, B. Mariana, R. K. Sanjaya, and D. Hermanto, "Polyelectrolyte complex (PEC) film based on chitosan as potential edible films and their antibacterial activity test," *IOP Conference Series: Materials Science and Engineering*, vol. 959, no. 1, Article ID 012009, 2020.